Journal of Biomechanics 49 (2016) 3230–3237

Contents lists available at ScienceDirect

Journal of Biomechanics

journal homepage: www.elsevier.com/locate/jbiomech
www.JBiomech.com

Hip and ankle responses for reactive balance emerge from varying priorities to reduce effort and kinematic excursion: A simulation study

Chris S. Versteeg, Lena H. Ting, Jessica L. Allen *

The Wallace H. Coulter Department of Biomedical Engineering, Emory University and Georgia Institute of Technology, Atlanta, GA, USA

ARTICLE INFO

Article history:
Accepted 2 August 2016

Keywords:
Forward dynamics
Posture
Kinematics
Simulation

ABSTRACT

Although standing balance is important in many daily activities, there has been little effort in developing detailed musculoskeletal models and simulations of balance control compared to other whole-body motor activities. Our objective was to develop a musculoskeletal model of human balance that can be used to predict movement patterns in reactive balance control. Similar to prior studies using torque-driven models, we investigated how movement patterns during a reactive balance response are affected by high-level task goals (e.g., reducing center-of-mass movement, maintaining vertical trunk orientation, and minimizing effort). We generated 23 forward dynamics simulations where optimal muscle excitations were found using cost functions with different weights on minimizing these high-level goals. Variations in hip and ankle angles observed experimentally (peak hip flexion = 7.9 – 53.1°, peak dorsiflexion = 0.5 – 4.7°) could be predicted by varying the priority of these high-level goals. More specifically, minimizing center-of-mass motion produced a hip strategy (peak hip flexion and ankle dorsiflexion angles of 45.5° and 2.3°, respectively) and the response shifted towards an ankle strategy as the priority to keep the trunk vertical was increased (peak hip and ankle angles of 13.7° and 8.5°, respectively). We also found that increasing the priority to minimize muscle stress always favors a hip strategy. These results are similar to those from sagittal-plane torque-driven models. Our muscle-actuated model facilitates the investigation of neuromechanical interactions governing reactive balance control to predict muscle activity and movement patterns based on interactions between neuromechanical elements such as spinal reflexes, muscle short-range stiffness, and task-level sensorimotor feedback.

1. Introduction

The purpose of this study was to develop a detailed musculoskeletal model of human balance that can be used to test hypotheses about principles of muscle coordination in reactive balance. Detailed musculoskeletal models combined with dynamic simulations can be used to study the relationship between muscle coordination and resulting movements. Although standing balance is of critical importance in many activities of daily living, there has been little effort in developing detailed musculoskeletal models and simulations of balance control compared to other whole-body motor activities such as walking (Anderson and Pandy, 2003; Liu et al., 2008; Neptune et al., 2008; Thelen and Anderson, 2006; Winby et al., 2009), running (Dorn et al., 2012; Hamner et al., 2010; Sasaki and Neptune, 2006), jumping (Anderson and Pandy, 1999; Bobbert and van Soest, 2001; Pandy and Zajac, 1991; Spagele et al., 1999), and cycling (Neptune and Hull, 1998; Raasch et al., 1997; Umberger et al., 2006).

Most computer modeling efforts in balance control have utilized predictive torque-driven models to investigate sensorimotor control of balance without regard for muscle coordination. They primarily focus on predicting experimental results from reactive balance responses, where an individual must maintain standing balance during support-surface perturbations involving either translation or rotation (e.g., Horak and Nashner, 1986; Torres-Oviedo and Ting, 2010). These joint torque-driven models range from simple one degree-of-freedom (DoF) inverted pendulums (ankle, e.g., Peterka, 2002, 2003) to multi-segmental inverted pendulums with two (hip and ankle, e.g., Kuo, 1995, 2005) and three DoF (hip, knee and ankle, e.g., van der Kooij et al., 1999, 2001) and can predict overall body movement when regulated by different sensory information (e.g. proprioceptive, vestibular and visual information). Only recently has a three-dimensional musculoskeletal model been used to simulate reactive balance, which was based on low-level stretch reflex-based control to minimize joint motion (Mansouri et al., 2015).

* Correspondence to: Emory Rehabilitation Hospital, Suite R150, 1441 Clifton Road, Atlanta, 30322 GA, USA.
E-mail address: jessica.allen@emory.edu (J.L. Allen).

http://dx.doi.org/10.1016/j.jbiomech.2016.08.007
0021-9290/

Evidence from both experimental and modeling approaches suggests that high-level task goals, such as reducing center-of-mass (CoM) excursion (Lockhart and Ting, 2007; Welch and Ting 2009, 2008), maintaining trunk orientation (Fung and Macpherson, 1995), stabilizing head motion (Nashner et al., 1988; Pozzo et al., 1990), and minimizing muscular effort (Lockhart and Ting, 2007) are important and may influence the type of response used in reactive balance. Experimentally-observed response strategies after perturbations to standing typically fall in a spectrum bounded by two extremes, a hip strategy and ankle strategy (Horak and Macpherson, 1996; Horak and Nashner, 1986; Nashner and Mccollum, 1985). The hip strategy, typically produced during unexpected or more difficult perturbation conditions, is characterized by large hip angle excursions. The ankle strategy, on the other hand, is often used in response to predictable or low difficulty perturbation conditions and involves minimal hip motion. Multilink torque-driven models can reproduce hip and ankle strategies to the same perturbation based on changing priorities of concurrent task-level goals, e.g. minimizing CoM, trunk, or joint angles (Kuo, 1995). It is not known how these goals can modulate response strategies in a three-dimensional muscle-driven model that has added complexity, such as the coordination of multiple muscles, out-of-plane joint motion, and muscle dynamics.

Here, we present predictive forward dynamics simulations of a detailed musculoskeletal model to identify how varying the priority of different high-level task goals alters kinematic response strategies in reactive balance. We incorporated physiologically realistic neural delays in muscle activity following the perturbation and used optimization methods to generate muscle activation patterns over time. Our primary objective was to demonstrate that we could generate a continuum of reactive balance responses in our three-dimensional muscle-driven model that is typical of those observed experimentally, i.e. hip vs. ankle strategy, by using a cost function with variable priority to minimize the high-level task goals of CoM and trunk orientation excursion. Our secondary objective was to examine how this relationship changes with increasing priority to minimize muscular effort.

2. Methods

We generated 23 forward dynamics simulations of a human musculoskeletal model during standing while subject to a backward support-surface perturbation (Fig. 1). Simulations minimized cost functions with different weights on CoM excursion, trunk orientation excursion, and muscle stress. Muscle excitation parameters were optimized using a simulated annealing algorithm.

2.1. Musculoskeletal model and simulation

A previously described 3D musculoskeletal model (Allen et al., 2014) with 23 DoF developed in SIMM (Musculographics, Inc.) was modified to simulate support-surface translations to standing balance (Fig. 1(A)). The model included rigid segments representing the trunk, pelvis, and two legs (thigh, shank, calcaneus and toes). The pelvis had six DoF (3 translations, 3 rotations). Hip joints were modeled as spherical joints and knee, ankle and subtalar joints were modeled as revolute joints. Passive torques representing connective tissues such as ligaments and tendons were applied at each joint based on previously reported data (Anderson, 1999). Because of the limited trunk musculature in the model, the trunk was rigidly attached to the pelvis. Ground contact was modeled using a planar joint between the toes and the ground with translational DoF in the anterior–posterior (AP) and mediolateral (ML) directions and rotational DoF along the vertical axis. To model support-surface translations the position, velocity and acceleration of the toe segment AP translation was prescribed by experimentally-measured translation kinematics from a backward support-surface perturbation with peak acceleration of 0.4 g, peak velocity of 35 cm/s, and total displacement of 10 cm (Fig. 1(B)).

The model was driven by 46 Hill-type musculotendon actuators per leg (Table 1). Muscle excitation signals were identical between legs. To account for neural conduction delays, constant muscle excitations during the first 100 ms after perturbation onset (Horak and Nashner, 1986; Nashner and Cordo, 1981) were found such that the simulation replicated previously observed experimental CoM kinematics during this period (e.g., Ting, 2007; Torres-Oviedo and Ting 2007, 2010). The shape of the muscle activity in the subsequent time period (100–1500 ms) was defined by cubic interpolation of 15 equally-spaced spline points (Fig. 1(D)). Muscle contraction and activation dynamics adhered to Hill-type muscle properties (Zajac, 1989) and muscle activation dynamics were modeled using a nonlinear first-order differential equation (Raasch et al., 1997). Polynomial equations were used to estimate musculotendon lengths and moment arms (Menegaldo et al., 2004) and dynamics of the forward simulation were computed through SD/FAST (PTC).

2.2. Optimization for strategy selection

To investigate how placing priority on controlling different high-level task goals affects reactive balance responses, simulations were generated using a simulated annealing algorithm (Goffe et al., 1994) that modified muscle excitation parameters to satisfy 23 different cost functions. The weights of each term in the cost function were varied to change their relative priorities (Table 2):

$$J = k_x \sum_t x(t)^2 + k_\theta \sum_t \theta(t)^2 + k_\mu \sum_t \sum_{j=1}^{nmus} \mu_j(t)^2 + \sum_{t=1485ms}^{1500ms} \left(k_{x_f} x(t)^2 + k_{\dot{x}_f} \dot{x}(t)^2 + k_{\ddot{x}_f} \ddot{x}(t)^2 + k_{\theta_f} \theta(t)^2 + k_{\omega_f} \omega(t)^2 \right)$$

The first term of this equation minimizes CoM excursion, where x represents AP CoM displacement from initial position. The second term minimizes trunk orientation excursion, where θ represents the angle of the trunk with respect to vertical. The third term minimizes muscle stress, where u_j is the activation level of muscle j. For each term, the contribution to the overall cost was weighted by a factor k that was varied to investigate the effects of changing priority of postural response goals (see Table 2 and below for more detail). The final term ensured the simulation ended in an upright, semi-static final position and summed CoM and trunk motion over the last 15 ms. An optimized behavior was considered acceptable if the model ended with terminal CoM velocity ($\dot{x}_f$) within ± 1 cm/s, CoM position (x_f) within ± 0.5 cm from the original upright standing posture, and trunk orientation (θ_f) with respect to gravity within ± 1 degrees. Terminal weighting parameters were held constant through all trials (Table 2).

Three sets of simulations were generated. The resulting peak CoM excursion, trunk orientation excursion, and hip, knee, and ankle angles were compared across simulations within each set.

1. Effect of minimizing CoM vs. trunk orientation excursion: To minimize CoM excursion, the weight for trunk orientation was set to zero ($k_\theta = 0$) and CoM and muscle stress weights (k_x and k_u) were set to 20 cm^{-1} and 0.005, respectively (Table 2, Set 1). To minimize trunk orientation excursion, CoM weight (k_x) was set to zero and trunk orientation and muscle stress weights (k_θ and k_u) were set to 500 $rads^{-1}$ and 0.005, respectively (Table 2, Set 2). Randomized spline parameters were used for initial muscle excitations.
2. Effect of varying the relative priority of CoM and trunk orientation excursions: Cost function weights (k_x, k_θ) were used as a proxy for task-level control priority. CoM excursion weight (k_x) was set to 20 cm^{-1} while trunk orientation weight was varied (k_θ = 10, 50, 100, 200, 300, 400, and 500 $rads^{-1}$) (Table 2, Set 2). Muscle stress weight (k_u) was set to 0.005. To place the initial guesses in the appropriate neighborhood and speed up convergence to the optimal solution, the muscle excitations were initialized with the excitations from (1)
3. Effect of minimizing muscle stress: We used the same seven trunk orientation and CoM excursion weights as in (3) and varied muscle stress weights (k_u) (Table 2, Set 3). We chose three stress weights representing low priority, normal priority, and high priority (k_u = 0.0005, 0.005, 0.05 respectively). Each optimization was initialized with the best muscle excitations from (2) to place the initial guesses in the appropriate neighborhood and speed up convergence to the optimal solution.

2.3. Experimental data for validation

We collected kinematics from one individual (male, 36 years old) of similar height and weight (177.0 cm, 75.0 kg) as the model (180.0 cm, 71.2 kg). The protocol was approved by the Georgia Institute of Technology Institutional Review Board and informed consent was obtained prior to data collection. The subject stood on two force-plates installed in a moveable platform and was exposed to a series of AP ramp-and-hold perturbations (peak acceleration, velocity and total displacement of 0.4 g, 35 cm/s, and 10 cm, respectively). With arms crossed against the chest, the subject was instructed to maintain balance while keeping the feet in place. The subject was first habituated to 20 forward perturbations and then unexpectedly given a backward perturbation. We then allowed the subject to adapt over 20 repeated trials in the backward direction. This was repeated three times for a total of 60 identical backwards perturbations. Body segment kinematics were collected at 120 Hz using an eight-camera motion capture system (Vicon) and custom 25-marker set that included head-arm-trunk, thigh, shank and foot segments. Kinematic data was low-pass filtered at 30 Hz. CoM kinematics were

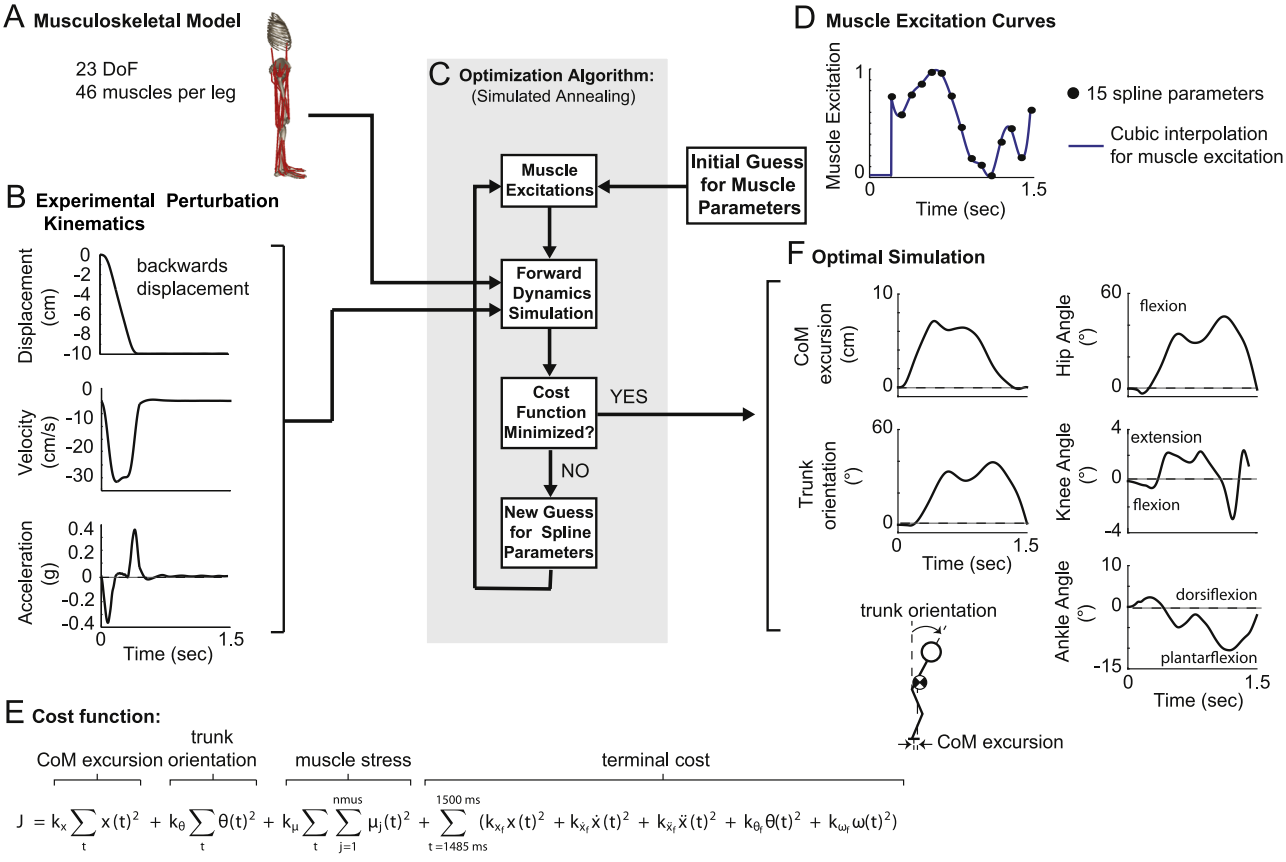

Fig. 1. Overview of simulation methods. (A) The forward dynamics simulations used a detailed musculoskeletal model with 23 degrees-of-freedom (DoF) and 46 muscles per leg. (B) Translation of the support-surface was achieved by prescribing the displacement, velocity, and acceleration of the anterior–posterior translation of the toe segment of the model using experimentally measured values. (C) Optimal muscle excitation parameters were found using a simulated annealing algorithm. (D) Muscle excitation signals were identical across legs and were not allowed to change for 100 ms after perturbation onset to account of neural conduction delays. The shape of the muscle excitation in the subsequent time period was defined by cubic interpolation of 15 equally-spaced spline points for a total simulation duration of 1.5 s. (E) The cost function included terms for minimizing center-of-mass excursion, trunk orientation excursion, and muscle stress. The weights for each of these three terms (k's) were varied to determine the effect of each parameter (see Table 2 for values). A terminal cost was also included that brought the model back to its initial state at the end of the simulation. (F) Once the optimization converged, center-of-mass excursion, trunk orientation, and hip, knee, and ankle angles were used to characterize the response and compared across each resulting simulation.

Table 1
Muscles included in the musculoskeletal model.

Gluteus medius 1	Gracilis
Gluteus medius 2	Quadratus femoris
Gluteus medius 3	Gemellus
Gluteus minimus 1	Piriformis
Gluteus minimus 2	Rectus femoris
Gluteus minimus 3	Vastus medialis
Gluteus maximus 1	Vastus intermedius
Gluteus maximus 2	Vastus lateralis
Gluteus maximus 3	Medial gastrocnemius
Adductor magnus 1	Lateral gastrocnemius
Adductor magnus 2	Soleus
Adductor magnus 3	Tibialis posterior
Adductor longus	Flexor digitorum longus
Adductor brevis	Flexor hallicus longus
Sartorius	Tibialis anterior
Iliacus	Peroneus brevis
Psoas	Peroneus longus
Tensor fascia lata	Peroneus tertius
Pectineus	Extensor digitorum longus
Semimembranosus	Extensor hallicus longus
Semitendinosus	Internal oblique
Biceps femoris long head	External oblique
Biceps femoris short head	Erector spinae

calculated from kinematic data using a weighted-sums approach (Winter 1990). Trunk orientation was calculated as the angle from vertical of the vector from the markers placed on the posterior iliac spine to the marker placed on C7.

3. Results

Greater hip and trunk motion were generated when minimizing only CoM versus trunk orientation excursion (simulation set 1, Fig. 2). Peak CoM excursion was lower when minimizing AP CoM compared to minimizing trunk orientation excursion (7.1 versus 7.9 cm; Fig. 2(A), solid red versus dashed blue line). Peak trunk orientation (Fig. 2(B)) was 39.4° versus 17.5° and peak hip flexion was 45.5° versus 13.7° (Fig. 2(C)) when minimizing CoM versus trunk orientation excursion. Peak ankle angle (Fig. 2(D)) was smaller and in the opposite direction when minimizing CoM excursion (10.5° ankle plantarflexion) versus trunk orientation (8.5° ankle dorsiflexion). These values were similar to the range of responses observed experimentally (Fig. 2, gray bars; peak CoM = 6.6–8.3 cm, peak trunk orientation = 23.0–54.2°, peak hip angle = 7.9–53.1°, peak dorsiflexion angle = 0.5–4.7°, peak plantarflexion angle = 1.4–13.1°).

When both CoM and trunk orientation excursion were differentially weighted (simulation set 2, Table 2), a spectrum of kinematic responses was produced that were intermediate to the two cases presented above. As expected, with increasing weights on trunk orientation, peak CoM increased (from 7.1 cm to 8.1 cm; Fig. 3(A), dashed red line) and peak trunk orientation decreased (39.8° to 25.1°, Fig. 3(A), solid blue line). Peak hip angle also decreased (44.6° to 26.3, Fig. 3(B), solid orange line) with minimal

Table 2
Cost function weights used in each optimization. The weights for CoM and trunk orientation were chosen to account for unit differences. The weights of 20 cm^{-1} and 100 rad^{-1} (simulation set 2, condition 3) result in approximately equal priority to minimize CoM and trunk orientation deviation, respectively. For sets 3 and 4 our range in CoM:trunk weights goes from approximately 10:1–1:10. The same terminal weights were used across all optimizations. These were set such that their total contributions were on the same order of magnitude as total CoM+trunk cost. Similarly, the initial stress weight was also set such that total stress contribution was on a similar order of magnitude as the total CoM+trunk cost over the simulation duration.

Cost function weights						
Set	Purpose	CoM (cm^{-1})	Trunk orientation (rad^{-1})	Muscle stress (Pa^{-1})	**Terminal weights** (applied to all cost functions)	
1	CoM excursion control Trunk orientation control	20 0	0 500	0.005 0.005	AP CoM position (k_{xf}, cm^{-1}) AP CoM velocity ($K_{\dot{x}_f}$, s/cm)	1×10^4 1×10^5
2	Relative priority of CoM excursion and trunk orientation control	20	Cond1: 10 Cond2: 50 Cond3: 100 Cond4: 200 Cond5: 300 Cond6: 400 Cond7: 500	0.005	AP CoM acceleration ($K_{\ddot{x}_f}$, s2/cm) Trunk angle ($K_{\theta f}$, rad^{-1}) Trunk angular velocity ($K_{\omega f}$, s/rad^{-1})	1.0 2×10^4 1×10^8
3	Effect of minimizing muscle stress	Same conditions as in set 3		0.0005 (low) 0.005 (med) 0.05 (high)		

changes in peak knee (3.3–3.4°, Fig. 3(B), dotted black line) and ankle angles (2.6–5.8°, Fig. 3(B), dashed purple line).

Increasing the priority to minimize muscle stress (simulation set 3) shifted the response towards more of a hip strategy, with the extent of this shift increasing as the priority to minimize trunk orientation excursion was increased (Fig. 4). Compared to the medium priority simulations, the average muscle stress was reduced by 18.9% and increased by 12.7% for the high and low priority simulations, respectively (Fig. 4(E)). There was no consistent change in peak CoM (Fig. 4(A)) or peak ankle angle (Fig. 4(D)) related to changes in the priority to minimize muscle stress. In contrast, as the priority to minimize muscle stress increased peak trunk orientation and hip angle increased across all combinations of CoM and trunk orientation excursion weights (Fig. 4(B) and (C)). The value of this change depended on the relative priority of minimizing trunk orientation versus CoM excursion. When the ratio of trunk orientation to CoM excursion weights was low, the increase in the peak hip and trunk angles with increasing priority to minimize muscle stress was also low (e.g., in Cond1 trunk angle increased only 1.4° and 0.9° when the priority to minimize muscle stress increased from low to medium to high). Conversely, when the ratio of trunk orientation to CoM excursion weights was high, the increase in peak hip and trunk angles was higher with increasing priority to minimize muscle stress (e.g., in Cond7 trunk angle increased 9.0° and 4.7°).

4. Discussion

Our results demonstrate that a 3D model of balance driven by muscle actuation to achieve high-level task goals can reasonably reproduce a range of reactive balance response to backwards support-surface perturbations. Based on different high-level task goals, our model reproduced a continuum of kinematic responses to identical perturbations that resemble experimentally-observed variations in hip and ankle strategy combinations. Experimentally, the response to a perturbation to standing balance can lie along a continuum defined by hip and ankle responses (Horak and Macpherson, 1996). The degree of hip angle excursion elicited can depend on both the characteristics of the perturbations (Welch and Ting, 2009) as well as recent prior exposure (Horak and Nashner, 1986; Welch and Ting, 2014). Similar to predictive simulations using sagittal-plane models controlled by joint torques during a lean-and-release paradigm (Kuo, 1995), we demonstrated that minimizing CoM excursion alone produced simulations with large hip and trunk angle deviations that resemble experimentally-observed hip strategies. Conversely, minimizing trunk orientation deviation produced simulations with small joint angle excursions at all joints, similar to observed ankle strategies. Moreover, transitioning from high priority to minimize CoM excursion to high priority to reduce trunk orientation excursion gradually shifts the response from a hip to an ankle strategy. Previous attempts at modeling reactive balance using 3D musculoskeletal models have focused on minimizing low-level goals such as individual joint motion that are biased towards ankle strategies and unable to produce the large joint motions inherent in the hip strategy (e.g., Mansouri et al., 2015).

The predictive model presented here will allow us to explore why response strategies to the same perturbation vary both within and across individuals in the context of high-level task goals. We found that the "optimal" response strategy was different depending on the relative priority of high-level goals. This priority change may occur on a relatively short timescale in healthy individuals, such as shifts from hip to ankle strategy that are observed experimentally over repeated identical trials (Fig. 5; Horak et al., 1989; Welch and Ting, 2014). Based on our simulation results, a potential mechanism for this shift towards an ankle strategy could be increased priority to maintain vertical trunk orientation. Upon first perturbation exposure the main priority may simply be not to fall down (i.e. ensure CoM does not exceed base of support). As an individual then adapts over subsequent perturbations other high-level goals, such as trunk orientation, may be optimized. Similar priority changes may also occur more rapidly, such as when switching from standing on a wide to a narrow base (Horak and Nashner, 1986) in which immediate increases in hip strategy response occur. Moreover, dancers have been shown to prioritize a vertical trunk orientation to a greater extent than non-dancers (Massion, 1992), suggesting that the set-point of these priorities may vary by population and/or life experience.

A novel finding of our simulations is that the effect of increasing priority to reduce effort is mediated by the relative priority to reduce vertical trunk orientation versus CoM excursion. Consistent with prior modeling studies that suggest a hip strategy is always more favorable than an ankle strategy (Kuo and Zajac, 1993), increasing the priority to minimize muscle stress resulted in increased trunk orientation and hip angles across all simulated

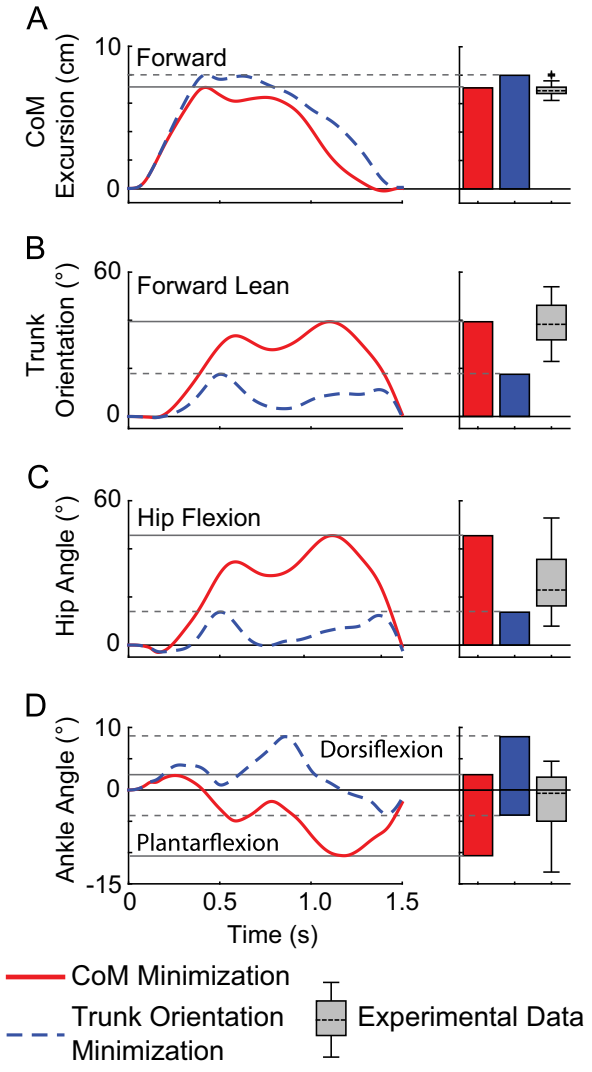

Fig. 2. Simulated kinematics when minimizing only center-of-mass versus only trunk orientation excursion. In response to identical perturbations, minimizing center-of-mass (CoM) versus trunk orientation excursion produced very different responses. The time-course of the simulated response (left panels) and peak values (right panels) are shown for (A) CoM excursion, (B) trunk orientation, (C) hip angle, and (D) ankle angle. Greater hip and trunk motion and smaller CoM excursion were generated when minimizing CoM excursion only (red solid line) versus trunk orientation excursion only (blue dashed line). Ankle deviations were small in both cases, but were in opposite directions (plantarflexion vs. dorsiflexion). The simulated responses were generally in agreement with the range observed experimentally in an individual of a height and mass similar to the model that was subjected to sixty perturbations of identical magnitude as the simulated perturbations (gray box plots in right panel). (For interpretation of the references to color in this figure legend, the reader is referred to the web version of this article.)

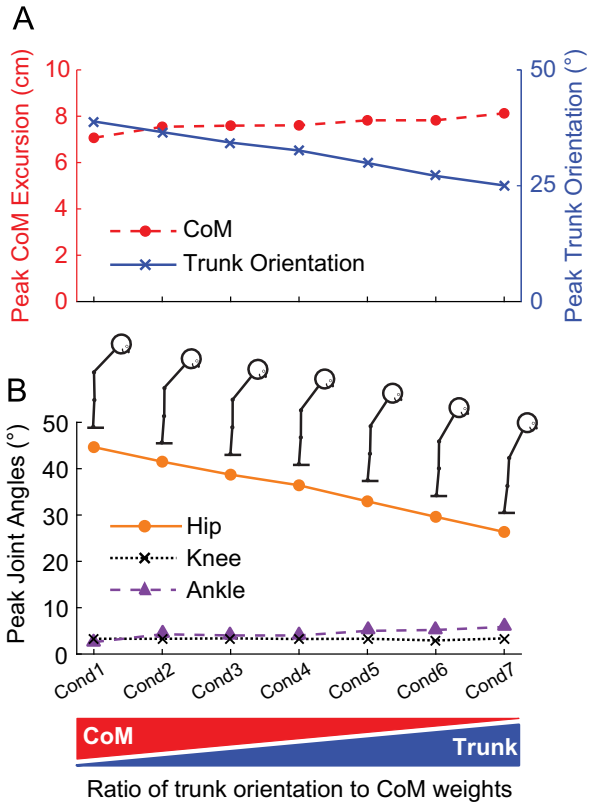

Fig. 3. Effect of varying priorities to minimize center-of-mass and trunk orientation excursion. When the priority to minimize both center-of-mass (CoM) and trunk orientation excursion were differentially weighted, a spectrum of kinematic patterns were produced that were intermediate to those found in simulations minimizing only CoM or trunk orientation excursion. As the relative weight to minimize trunk orientation versus CoM excursion increased (left to right): (A) peak trunk orientation (solid blue line) decreased while peak CoM (dashed red line) increased and (B) peak hip angle decreased (solid orange line) while ankle dorsiflexor angle (dashed purple lines) increased slightly, with no discernable changes in peak knee angle (dotted black line). (For interpretation of the references to color in this figure legend, the reader is referred to the web version of this article.)

conditions (Fig. 4). However, these increases were small when CoM excursion was weighted highest and became larger as the priority to reduce trunk orientation was increased. This suggests that there may be multiple muscle recruitment patterns that similarly minimize CoM excursion with varying levels of effort, whereas maintaining vertical trunk orientation may require specific and energetically costly muscle recruitment patterns.

This study represents a first step in developing a predictive model for examining how muscles control perturbations to standing balance. This modeling approach will allow us to alter musculoskeletal parameters (e.g. muscle strength and dynamics) to represent either more athletic or frail individuals in order to predict how training and/or neuromuscular impairments affect the control of balance. While our model represents a step up from the sagittal-plane torque-driven models typically used to model reactive balance responses, we made several assumptions that must be further developed to expand its utility beyond the backwards support-surface perturbations presented here. First, we made two model simplifications. The joint between the pelvis and trunk was locked because of limited trunk musculature. This choice is justified for a backwards perturbation because motion between the pelvis and trunk in the sagittal plane is typically very small with minimal non-sagittal-plane trunk motion. We also modeled ground contact using a planar toe-ground joint with fixed vertical toe position. The fixed toe vertical position was justified because there is typically minimal vertical toe motion in a backward perturbation. Post-hoc analyses show that peak vertical reaction forces of the toe-ground joint (range = 129.4 N – 168.3 N) are within the fluctuations of $\pm$200 N observed experimentally, confirming these are feet-in-place responses as desired. To examine other perturbations in which we cannot assume minimal trunk-pelvis motion or toe-movement (e.g. toe lifting is an issue in forward perturbations), more realistic trunk musculature and ground contact model (e.g., surface contact model: Lopes et al., 2016, a bed of springs: Neptune et al., 2000, elastic foundation mesh-based model: Seth et al., 2011) must be implemented. Second, we made two simplifications regarding muscle excitation patterns: an identical neural delay period of 100 ms for all muscles and identical muscle excitation patterns between legs. Although there may be slight differences in the minimum latency of muscle

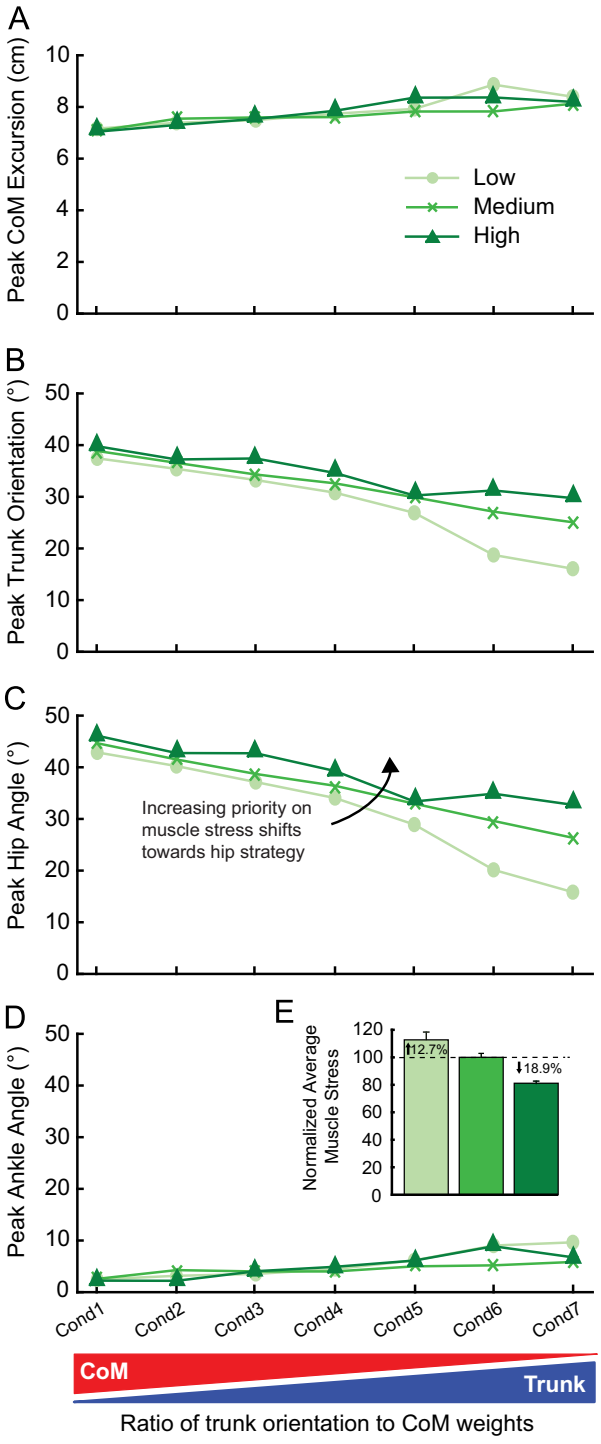

Fig. 4. Effect of minimizing muscle stress on response kinematics. The peak (A) center-of-mass (CoM) excursion, (B) trunk orientation, (C) hip angle, and (D) ankle angle are shown across increasing (left to right) ratios of priority to minimize trunk orientation vs. CoM excursion (*x*-axis, increasing trunk to CoM weight ratio) for low (light green circles), medium (green x's), and high (dark green triangles) priority to minimize muscle stress. As the priority to minimize muscle stress increased (light to dark lines): (A) peak CoM showed no consistent change, (B) peak trunk orientation and (C) peak hip angle increased and (D) peak ankle angle had minimal changes across all trunk to CoM weight ratios. The extent of these changes in trunk and hip angles with increasing priority to minimize muscle stress was larger when the priority to minimize trunk orientation was also high (e.g. Cond7 vs Cond1). (E) As expected, average muscle stress (normalized to the medium condition) decreased as the priority to minimize muscle stress was increased. (For interpretation of the references to color in this figure legend, the reader is referred to the web version of this article.)

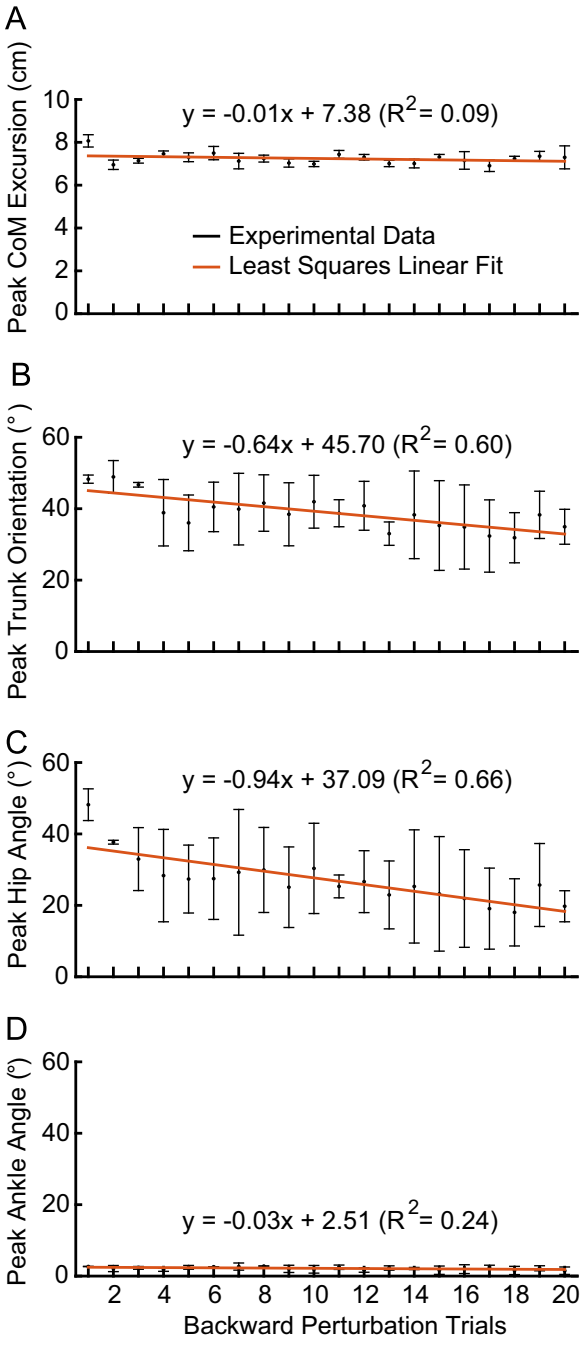

Fig. 5. Effect of repeated perturbations on experimental kinematic response. The peak (A) center-of-mass (CoM) excursion, (B) trunk orientation, (C) hip angle, and (D) ankle angle are shown across sets of repeated perturbations of identical magnitude (left to right). Experimental kinematics were collected from one individual (male, 36 years old) of similar height and weight (177.0 cm, 75.0 kg) as the model (180.0 cm, 71.2 kg). The subject was first habituated to 20 forward perturbations and then unexpectedly given a series of 20 backward perturbations of identical magnitude as that applied in the simulations. This was repeated a total of three times. Only the response to the backward perturbations are shown. Post-hoc analyses using least-squares linear fits (thick red lines) were used to examine changes in experimental kinematics (thin black lines) over repeated backwards perturbations. There was a trend for the response strategy to shift towards an ankle strategy as the subject adapted to the perturbations with a reduction in both peak (B) trunk orientation and (C) hip angle. (For interpretation of the references to color in this figure legend, the reader is referred to the web version of this article.)

responses ranging from 80–120 ms (Nashner and Cordo, 1981), we do not believe this would alter the qualitative results of the current study but may be important to include as we begin to examine populations with altered neural delays (e.g., stroke, Marigold and Eng, 2006). While having identical muscle excitations between legs likely provides some inherent stability in the mediolateral plane, this constraint was based on the observation that many individuals utilize similar patterns of muscle recruitment between legs in response to a backwards perturbation. To examine the response to different perturbation directions this constraint must be removed. Finally, the terminal constraint that ensures the model returns upright was implemented by specifying a priori the overall simulation time. We set the overall simulation time (1.5 s) based on observed response times in our experimental data, but future development will allow this to vary.

This study establishes a new computational framework for facilitating the investigation of neuromechanical interactions governing balance control. Here we focused on implementing control of high-level task goals, which can be combined with models of other neuromechanical elements contributing to balance control such as spinal reflexes, muscle short-range stiffness, and task-level sensorimotor feedback (Ting 2007, Ting et al., 2009). Spinal reflexes and short-range stiffness likely contribute in the first 100 ms after a perturbation, which we modeled here as a period of constant muscle excitation. While our model currently reproduces the initial passive kinematics of the body, adding reflexes and short-range stiffness would allow us to investigate the effects of altered short-range stiffness or short-latency reflexes that occur with aging or impairment. Spinal reflexes are insufficient to generally explain the entire postural response (Bunderson et al., 2010; Nashner, 1976; Ting and Macpherson, 2004), and we previously demonstrated that a simple inverted pendulum model can be controlled using sensorimotor feedback of CoM kinematics (Lockhart and Ting, 2007; Welch and Ting, 2009, 2008). Our results suggest that sensorimotor feedback of both CoM and trunk variables will be necessary to stabilize complex musculoskeletal models with explicit hip, knee, and ankle joints that have multiple degrees of freedom and are more comparable to human anatomy.

Conflict of interest statement

We wish to confirm that there are no known conflicts of interest associated with this publication and there has been no significant financial support for this work that could have influenced its outcome.

Acknowledgments

CSV was supported by NIH Training Grant R90DA033462 and a Presidential Undergraduate Research Award from the Georgia Institute of Technology. JLA was supported by NIH T32 NS007480 and F32 NS087775. NIH Grant HD46922 to LHT. NIH had no role in the design, performance, or interpretation of the study.

References

Allen, J.L., Kautz, S.A., Neptune, R.R., 2014. Forward propulsion asymmetry is indicative of changes in plantarflexor coordination during walking in individuals with post-stroke hemiparesis. Clin. Biomech. 29, 780–786.

Anderson, F.C., 1999. A Dynamic Optimization Solution for a Complete Cycle of Normal Gait (Doctoral Dissertation). The University of Texas at Austin.

Anderson, F.C., Pandy, M.G., 1999. A Dynamic Optimization solution for vertical jumping in three dimensions. Comput. Methods Biomech. Biomed. Eng. 2, 201–231.

Anderson, F.C., Pandy, M.G., 2003. Individual muscle contributions to support in normal walking. Gait Posture 17, 159–169.

Bobbert, M.F., van Soest, A.J., 2001. Why do people jump the way they do? Exerc. Sport Sci. Rev. 29, 95–102.

Bunderson, N.E., McKay, J.L., Ting, L.H., Burkholder, T.J., 2010. Directional constraint of endpoint force emerges from hindlimb anatomy. J. Exp. Biol. 213, 2131–2141.

Dorn, T.W., Schache, A.G., Pandy, M.G., 2012. Muscular strategy shift in human running: dependence of running speed on hip and ankle muscle performance. J. Exp. Biol. 215, 1944–1956.

Fung, J., Macpherson, J.M., 1995. Determinants of postural orientation in quadrupedal stance. J. Neurosci. 15, 1121–1131.

Goffe, W.L., Ferrier, G.D., Rogers, J., 1994. Global optimization of statistical functions with simulated annealing. J. Econ. 60, 65–99.

Hamner, S.R., Seth, A., Delp, S.L., 2010. Muscle contributions to propulsion and support during running. J. Biomech. 43, 2709–2716.

Horak, F.B., Diener, H.C., Nashner, L.M., 1989. Influence of central set on human postural responses. J. Neurophysiol. 62, 841–853.

Horak, F.B., Macpherson, J.M., 1996. Postural orientation and equilibrium. In: Handbook of Physiology, Section 12. American Physiological Society, New York, pp. 255–92.

Horak, F.B., Nashner, L.M., 1986. Central programming of postural movements: adaptation to altered support-surface configurations. J. Neurophysiol. 55, 1369–1381.

Kuo, A.D., 1995. An optimal control model for analyzing human postural balance. IEEE Trans. Biomed. Eng. 42, 87–101.

Kuo, A.D., 2005. An optimal state estimation model of sensory integration in human postural balance. J. Neural Eng. 2, S235–S249.

Kuo, A.D., Zajac, F.E., 1993. Human standing posture: multi-joint movement strategies based on biomechanical constraints. Prog. Brain Res. 97, 349–358.

Liu, M.Q., Anderson, F.C., Schwartz, M.H., Delp, S.L., 2008. Muscle contributions to support and progression over a range of walking speeds. J. Biomech. 41, 3243–3252.

Lockhart, D.B., Ting, L.H., 2007. Optimal sensorimotor transformations for balance. Nat. Neurosci. 10, 1329–1336.

Lopes, D.S., Neptune, R.R., Ambrosio, J.A., Silva, M.T., 2016. A superellipsoid-plane model for simulating foot-ground contact during human gait. Comput. Methods Biomech. Biomed. Eng. 19, 954–963.

Mansouri, M., Clark, A.E., Seth, A., Reinbolt, J.A., 2015. Rectus femoris transfer surgery affects balance recovery in children with cerebral palsy: a computer simulation study. Gait Posture 43, 24–30.

Marigold, D.S., Eng, J.J., 2006. Altered timing of postural reflexes contributes to falling in persons with chronic stroke. Exp. Brain Res. 171, 459–468.

Massion, J., 1992. Movement, posture and equilibrium: interaction and coordination. Prog. Neurobiol. 38, 35–56.

Menegaldo, L.L., de Toledo Fleury, A., Weber, H.I., 2004. Moment arms and musculotendon lengths estimation for a three-dimensional lower-limb model. J. Biomech. 37, 1447–1453.

Nashner, L.M., 1976. Adapting reflexes controlling the human posture. Exp. Brain Res. 26, 59–72.

Nashner, L.M., Cordo, P.J., 1981. Relation of automatic postural responses and reaction-time voluntary movements of human leg muscles. Exp. Brain Res. 43, 395–405.

Nashner, L.M., Mccollum, G., 1985. The organization of human postural movements - a formal basis and experimental synthesis. Behav. Brain Sci. 8, 135–150.

Nashner, L.M., Shupert, C.L., Horak, F.B., 1988. Head-trunk movement coordination in the standing posture. Prog. Brain Res. 76, 243–251.

Neptune, R.R., Hull, M.L., 1998. Evaluation of performance criteria for simulation of submaximal steady-state cycling using a forward dynamic model. J. Biomech. Eng. 120, 334–341.

Neptune, R.R., Sasaki, K., Kautz, S.A., 2008. The effect of walking speed on muscle function and mechanical energetics. Gait Posture 28, 135–143.

Neptune, R.R., Wright, I.C., Van Den Bogert, A.J., 2000. A method for numerical simulation of single limb ground contact events: application to heel-toe running. Comput. Methods Biomech. Biomed. Eng. 3, 321–334.

Pandy, M.G., Zajac, F.E., 1991. Optimal muscular coordination strategies for jumping. J. Biomech. 24, 1–10.

Peterka, R.J., 2002. Sensorimotor integration in human postural control. J. Neurophysiol. 88, 1097–1118.

Peterka, R.J., 2003. Simplifying the complexities of maintaining balance. IEEE Eng. Med. Biol. Mag. 22, 63–68.

Pozzo, T., Berthoz, A., Lefort, L., 1990. Head stabilization during various locomotor tasks in humans. I. normal subjects. Exp. Brain Res. 82, 97–106.

Raasch, C.C., Zajac, F.E., Ma, B., Levine, W.S., 1997. Muscle coordination of maximum-speed pedaling. J. Biomech. 30, 595–602.

Sasaki, K., Neptune, R.R., 2006. Muscle mechanical work and elastic energy utilization during walking and running near the preferred gait transition speed. Gait Posture 23, 383–390.

Seth, A., Sherman, M., Reinbolt, J.A., Delp, S.L., 2011. OpenSim: a musculoskeletal modeling and simulation framework for investigations and exchange. Proced. IUTAM 2, 212–232.

Spagele, T., Kistner, A., Gollhofer, A., 1999. Modelling, simulation and optimisation of a human vertical jump. J. Biomech. 32, 521–530.

Thelen, D.G., Anderson, F.C., 2006. Using computed muscle control to generate forward dynamic simulations of human walking from experimental data. J. Biomech. 39, 1107–1115.

Ting, L.H., 2007. Dimensional reduction in sensorimotor systems: a framework for understanding muscle coordination of posture. Prog. Brain Res. 165, 299–321.
Ting, L.H., Macpherson, J.M., 2004. Ratio of shear to load ground-reaction force may underlie the directional tuning of the automatic postural response to rotation and translation. J. Neurophysiol. 92, 808–823.
Ting, L.H., van Antwerp, K.W., Scrivens, J.E., McKay, J.L., Welch, T.D., Bingham, J.T., DeWeerth, S.P., 2009. Neuromechanical tuning of nonlinear postural control dynamics. Chaos 19, 026111.
Torres-Oviedo, G., Ting, L.H., 2007. Muscle synergies characterizing human postural responses. J. Neurophysiol. 98, 2144–2156.
Torres-Oviedo, G., Ting, L.H., 2010. Subject-specific muscle synergies in human balance control are consistent across different biomechanical contexts. J. Neurophysiol. 103, 3084–3098.
Umberger, B.R., Gerritsen, K.G., Martin, P.E., 2006. Muscle fiber type effects on energetically optimal cadences in cycling. J. Biomech. 39, 1472–1479.
van der Kooij, H., Jacobs, R., Koopman, B., Grootenboer, H., 1999. A multisensory integration model of human stance control. Biol. Cybern. 80, 299–308.
van der Kooij, H., Jacobs, R., Koopman, B., van der Helm, F., 2001. An adaptive model of sensory integration in a dynamic environment applied to human stance control. Biol. Cybern. 84, 103–115.
Welch, T.D., Ting, L.H., 2008. A feedback model reproduces muscle activity during human postural responses to support-surface translations. J. Neurophysiol. 99, 1032–1038.
Welch, T.D., Ting, L.H., 2009. A feedback model explains the differential scaling of human postural responses to perturbation acceleration and velocity. J. Neurophysiol. 101, 3294–3309.
Welch, T.D., Ting, L.H., 2014. Mechanisms of motor adaptation in reactive balance control. PLoS One 9, e96440.
Winby, C.R., Lloyd, D.G., Besier, T.F., Kirk, T.B., 2009. Muscle and external load contribution to knee joint contact loads during normal gait. J. Biomech. 42, 2294–2300.
Winter, D.A., 1990. Biomechanics and Motor Control of Human Movement, 2nd ed. John Wiley & Sons, New York.
Zajac, F.E., 1989. Muscle and tendon: properties, models, scaling, and application to biomechanics and motor control. Crit. Rev. Biomed. Eng. 17, 359–411.